Consequence of 2012 M_w 8.6 Northern Sumatra Earthquakes towards Sundaland Plate

Chien Zheng YONG, Paul DENYS, Christopher PEARSON, New Zealand

Key words: Sundaland plate, velocity field, geodesy, 2012 M_w 8.6 northern Sumatra doublet earthquakes

SUMMARY

The impact of postseismic decay has been concerned mostly with the edge of plate boundaries. But great earthquakes (larger than M8.0) can cause widespread postseismic decay in areas well beyond any recognised plate boundaries. The M_w 8.6 and 8.2 northern Sumatra doublet earthquakes occurred on 11 April 2012, near the intersection of the Indian, Australian and Sundaland plate, have caused an extensive coseismic offset and postseismic decay over the region. In this study, the long-term GPS time-series (1999 – 2014) suggests that the postseismic decay associated with the 2012 doublet earthquakes have had a significant effect on the eastern boundary of the Sundaland plate up to the western region of Peninsular Malaysia. Before the 2004 M_w 9.1 Aceh and 2005 M_w 8.6 Nias earthquakes, the average velocity of continuous GNSS sites in Peninsular Malaysia is moving 31 ± 2.1 mm/yr southeast relative to ITRF2008. The postseismic decay of these two great earthquakes have caused Peninsular Malaysia to slightly deviate into the south-southeast direction with a lower average velocity by 10 ± 5.5 mm/yr. After 2012 northern Sumatra earthquakes Peninsular Malaysia returns to its original course of motion before the 2004 and 2005 earthquakes, with slightly lower average velocity at 25 ± 2.4 mm/yr. In this paper, the GPS network and availability of data are summarised. Next, the GPS processing strategies and deformation analysis used in this study are discussed. The paper then focuses on the impact of coseismic and postseismic deformation of the 2012 M_w 8.6 and 8.2 northern Sumatra earthquakes towards Sundaland plate vectors. Lastly, a new rotation vector for Sundaland plate is defined in ITRF2008 by using 10 selected cGPS sites that are assumed to be located in the stable block, based on the 1999 – 2004 time-series data.

Consequence of 2012 M_w 8.6 Northern Sumatra Earthquakes towards Sundaland Plate

Chien Zheng YONG, Paul DENYS, Christopher PEARSON, New Zealand

1. INTRODUCTION

The Sundaland plate is the continental core of Southeast Asia (SEA), which is located in a tectonically complex region. In the north, the Sundaland plate is a coherent block that moves with respect to Eurasia continental plate and is partitioned from the Siberian platform. In the south, Sundaland is in direct contact with the Indian-Australian oceanic plate and several microblocks (Burma, Timor, Banda Sea, Molucca Sea, Bird heads, Philippine Sea, and Yangtze plate) (Figure 1), that form a sparse seismicity zone along the edge of plate.

The conjunction between the Sundaland plate and Indian-Australian plate, in particular, is a well-known megathrust that occasionally generates great earthquakes. The Indian-Australian oceanic plate is subducting beneath the Sundaland continental plate at a relative vector of 47 mm/yr N0° at the triple junction point of the Indian, Australian and Sundaland plates (90°E, 9°N). The relative vector increases towards the south from 55 mm/yr N10° at the equator near Nias Island to 63 mm/yr N14° south of the Sunda Strait (Socquet *et al.*, 2006; Simons *et al.*, 2007).

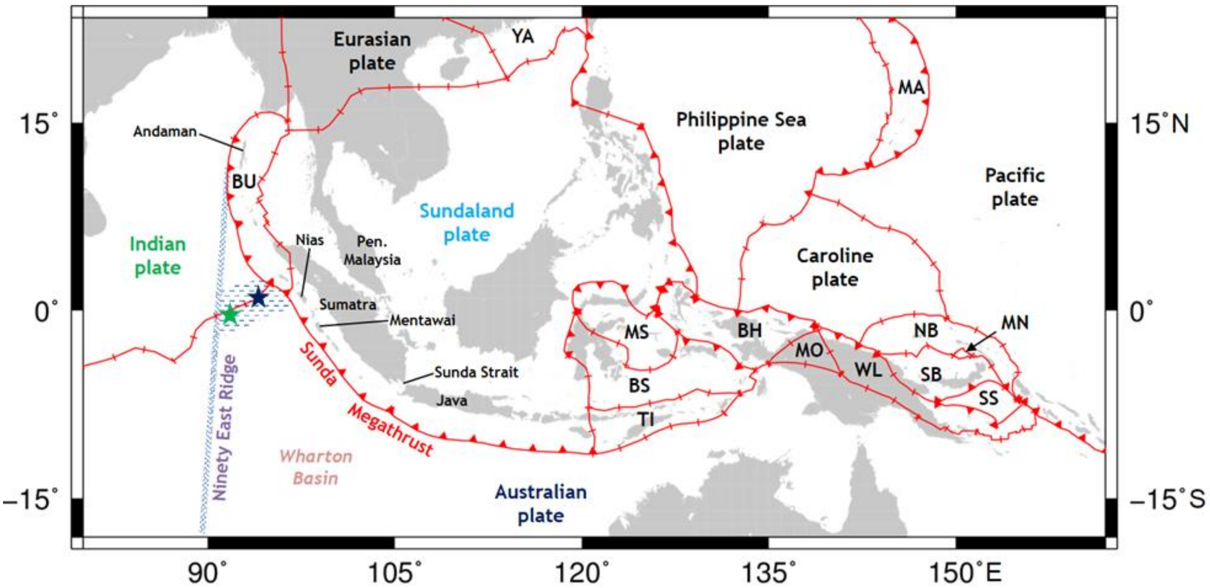

Figure 1: The plate boundaries of Sundaland plate with its surrounding plates as defined by Bird (2003). The blue star indicates the 2012 M_w 8.6 earthquake and the green star indicates the M_w 8.2 earthquake. The blue shades area shows the rupture region of the 2012 doublet earthquakes. Two-letter plate identifiers are: Birds Head (BH), Banda Sea (BS), Burma (BU), Mariana (MA), Manus (MN), Maoke (MO), Molucca Sea (MS), North Bismarck (NB), Timor (TI), South Bismarck (SB), Solomon Sea (SS), Woodlark (WL) and Yangtze (YA).

On 11 April 2012, two of the largest (M_w 8.6 and 8.2) strike-slip and intraplate earthquakes ever recorded by modern seismological instruments struck at the southwest of the Sunda megathrust within a period of a few hours. These strike-slip earthquakes are situated at the intra-oceanic plate region between the India plate and Australia plate that possibly involved a substantial lithospheric deformation that may eventually lead to the formation of a localised plate boundary (Duputel *et al.*, 2012). The left-lateral strike-slip earthquakes have induced a significant coseismic offset over the Sundaland plate over a region 2500 km from the rupture zone. Furthermore, the event has created a widespread postseismic deformation signal at the western margin of the Sundaland plate. Global Positioning System (GPS) measurements indicate that northern Sumatra and northwest Peninsula Malaysia are experiencing a larger postseismic decay amplitude compared to the central and southern regions.

In this paper, we describe the cGPS (continuous GPS) network and data availability and discuss the GPS processing strategies and deformation analysis used in this study. The paper then focuses on the discrepancy between the derived vectors and the predictions of global plate motion model, the Mid-Ocean Ridge Velocity (MORVEL), within Sundaland plate. Lastly, a new rotation vector for Sundaland plate is defined with respect to the International Terrestrial Reference Frame (ITRF) 2008, based on 10 selected cGPS sites that are located on the stable block. The coseismic and postseismic deformation of great earthquakes (M8 or greater) between year 1999 – 2014 are modelled and a new rotation vector of Sundaland plate is defined.

2. cGPS NETWORK

To study the plate vector of Sundaland, a large and dense cGPS network that spans over the SEA region is required because of the complexity of plate interior deformation. However, the global velocity models as described in Altamimi *et al.* (2012) and Kreemer *et al.* (2014) do not have sufficient spatio-temporal resolution to model the Sundaland plate vector. In this study, several national and regional GPS networks in the SEA region are merged to form a larger network of up to 143 GPS permanent sites: 96 Malaysian Real-Time Kinematic Network (MyRTKnet) and Malaysian Active GPS System (MASS) sites in Malaysia; 39 Sumatran GPS Array (SuGAr) sites in Indonesia; and one Philippine Active Geodetic Network (pageNET) in the Philippines (Figure 2). The data availability of GPS data per year is shown in Table 1.

The Indonesian sites, which are mainly located in the edge of Sundaland plate, have been widely studied by many researchers (Bock *et al.*, 2003; Kreemer *et al.*, 2014) but not the decade-long cGPS data from the MyRTKnet. Most of the Indonesian sites were subjected to site-dependent bias and local deformation while the Malaysian sites which are mainly located in the stable core of Sundaland plate are thus better able to define the Euler pole of Sundaland plate.

Table 1: Overview of the GPS data availability from 1999 - 2014

Network	# of sites	Year															
		1999	2000	2001	2002	2003	2004	2005	2006	2007	2008	2009	2010	2011	2012	2013	2014
MyRTKnet	78	-	-	-	-	-	27	27	27	71	78	79	78	78	78	78	78
MASS*	18	15	15	17	17	18	18	-	-	-	-	-	-	-	-		
SuGAr	46	2	2	2	8	8	16	27	31	31	36	32	41	39	40	41	40
pageNET	1	-	-	-	-	-	-	-	-	-	-	-	1	1	1	1	1
SUB-TOTAL	143	17	17	19	25	26	61	54	58	102	114	111	120	118	119	120	119
Regional IGS																	
PIMO	1	1	1	1	1	1	1	1	1	1	1	1	1	1	1	1	1
NTUS	1	1	1	1	1	1	1	1	1	1	1	1	1	1	1	1	1
CUSV	1	-	-	-	-	-	-	-	-	-	1	1	1	1	1	1	1
SUB-TOTAL	146	19	19	21	27	28	63	56	60	104	117	114	123	121	122	123	122
IGS	41	34	34	36	39	40	40	41	41	41	41	41	41	41	40	38	37
TOTAL	187	53	53	57	66	68	103	97	101	145	158	155	164	162	162	161	159

Note: MASS network marked with an asterisk indicate that all the GPS sites were either upgraded after 2007 to become the MyRTKnet sites or no longer in operation.

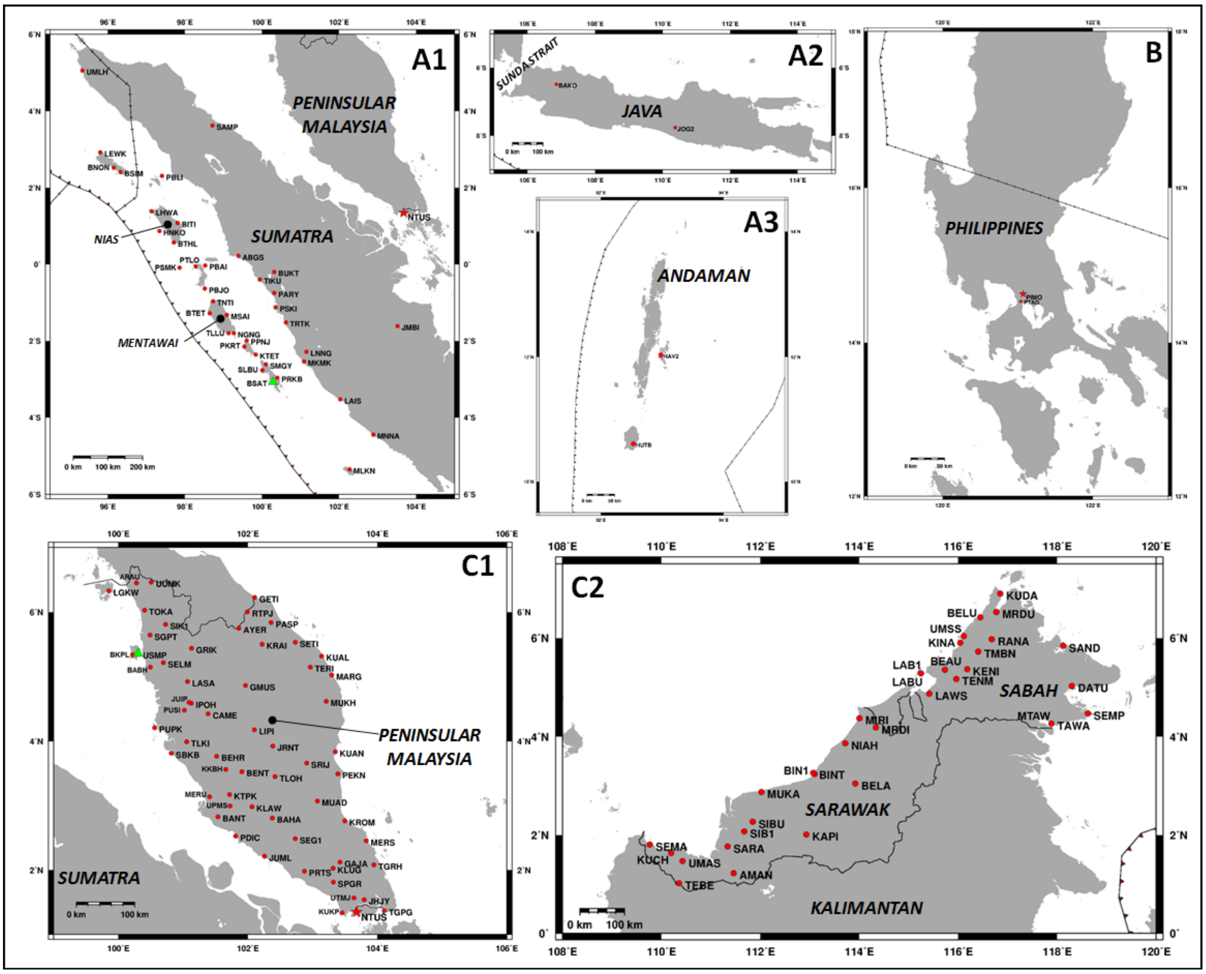

Figure 2: The GPS sites distribution in Southeast Asia used in this study. The five boxes designated the cGPS networks installed in each region: Indonesia – SuGAR network (consisting of A1: Sumatra, Nias and Mentawai Island, A2: Java Island and A3: Andaman Island); (B) the Philippines – pageNET; and Malaysia – MyRTKnet and MASS network (consisting of C1: Peninsular Malaysia and C2: Sabah and Sarawak).

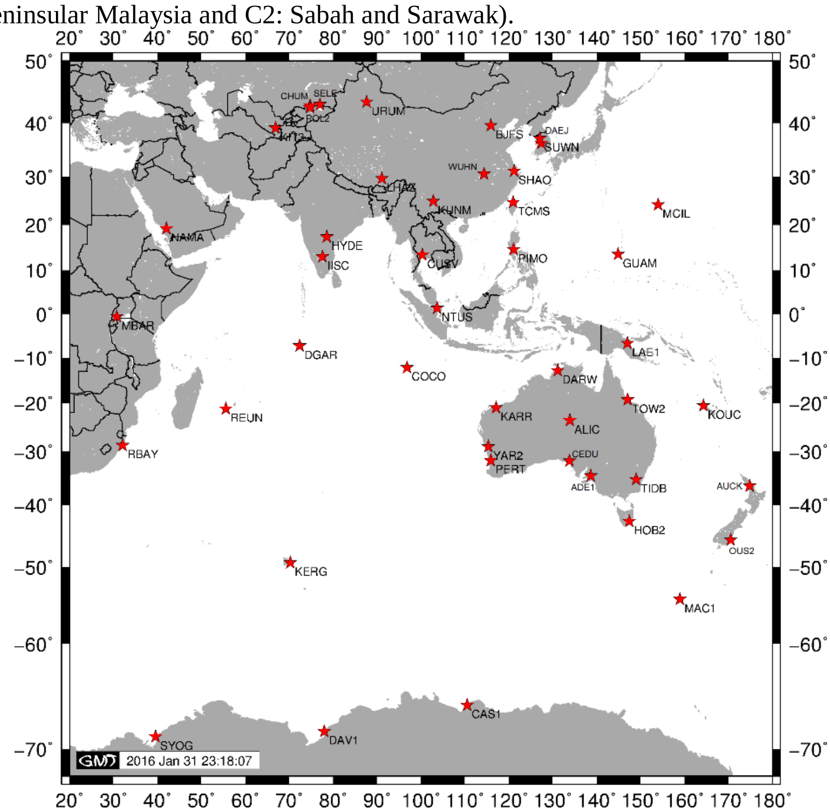

Figure 3: Distribution of IGS sites used in this study.

A global-and-regional distributed network consisting of 44 IGS sites are selected to represent the reference frame in ITRF2008 (Figure 3). These selected IGS sites are mostly located in stable zones (with linear GPS time-series) as defined in Altamimi *et al.*, (2012). However, some of the IGS sites are located close to plate boundaries or within deformation zones (*i.e.* COCO, DGAR and GUAM) that are included to improve the network distribution. Three regional IGS sites (NTUS, PIMO and CUSV) located within the Sundaland plate were excluded from the frame definition.

3. DATA ANALYSIS

The data processing of the IGS and regional cGPS sites were uniformly analysed using the Bernese software Version 5.2 (Dach *et al.*, 2007), a scientific multi-Global Navigation Satellite System (GNSS) data processing software developed at the Astronomical Institute of the University of Bern (AIUB). The double-differencing (DD) processing technique is applied in final coordinate estimation where differences of phase observables between two satellites and two stations are involved. This technique requires the generation of inter-site baselines, which were predefined in six clusters, by considering the baseline length and data availability (in space and time). The inhomogeneous data sources are unified in data processing, for instance, most cGPS network (global and regional) is in 30-second data interval except for the SuGAr network that is logged at 120-second data interval. The high level of water vapour in low-latitude regions is another critical challenge in GPS data processing (Musa *et al.*, 2011). The global mapping function (GMF), wet_GMF and dry_GMF, are introduced as an a priori tropospheric model (Boehm *et al.*, 2006), and the zenith path delay (ZPD) is estimated in every two-hour interval at each site. The summary of GPS data processing strategy is described in Table 2.

Table 2: Parameters setting and models for data processing

PROCESSING PARAMETERS	PROCESSING STRATEGIES
Input data	*Daily*
Processing software	*Bernese Version 5.2*
Processing technique	*Double-Differencing*
Network design	*OBS-MAX*
Elevation cut off angle	*10°*
Sampling rate	*30 – 120 sec*
Orbit / EOP	*3-day long-arc solution CO2 repro2 products (CODE) (1999.0 – 2013.9); CODE final orbit (2014.0-2014.9)*
Station coordinates	*Constrained to the ITRF2008*
Absolute antenna phase centre corrections	*PHASE COD.I08, SATELLIT.I08*
Ocean loading model	*FES2004* (Scherneck, 1991)
Planetary ephemeris	*DE405*
Ionosphere	*Double difference Ionosphere-free (IF) linear combination L3*
Ambiguities solution	*Fixed, resolved using QIF strategy*
A-priori model	*wet_GMF model (hydrostatic part) with dry_GMF mapping function*
Mapping Function	*wet_GMF mapping function (2 hour interval)*

In this study, the GPS velocity field is derived in terms of ITRF2008 from position time-series of up to 16 years. Each site velocity is extracted by linear regression of time-series from sites which signify steady-state motion. Overall, the range of the position root-mean-square (RMS) values are ±1 – 3 mm, ±1 – 4 mm, and ±5 – 9 mm for the northing, easting and up components, respectively (*e.g.* Figure 4). There are also some cGPS sites in the active deformation zone, particularly those located at the edge of plate boundary or active seismicity region like the Mentawai Islands, Sumatra and Andaman Islands, (Figure 2 – A1 and A3), having irregular time-series which are excluded from the GPS velocity field derivation (Figure 5).

The procedure we use to model the GPS velocity field allows us to correct for coseismic offset and postseismic decay amplitude caused by a series of great earthquakes since 1999. These include the 2004 M_w 9.1 Aceh, 2005 M_w 8.6 Nias, 2007 M_w 8.5 Bengkulu, and the most recent 2012 M_w 8.6 and 8.2 northern Sumatra earthquakes. Additionally, there are eight M_w 7.0 – 7.9 and fifteen M_w 6.0 – 6.9 earthquake events with small-to-moderate but measurable displacements which were modelled at a few sites. The long position time-series are providing important information in estimating the postseismic decay amplitude and duration of earthquakes events. Thus, a more accuracy velocity can be estimated for the GPS velocity field of Sundaland plate.

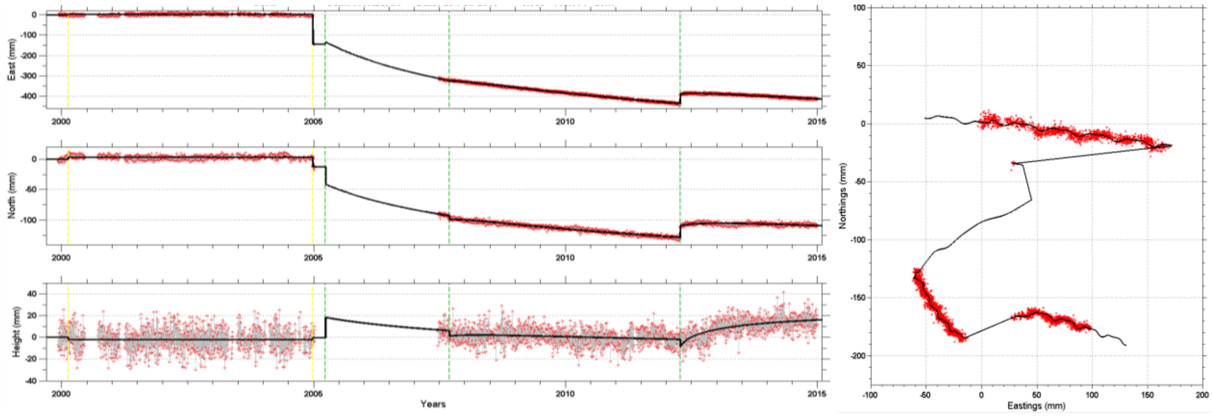

Figure 4: Time-series of station USMP. This Malaysian cGPS site was initially a MASS station installed in 1999 at *Universiti Sains Malaysia*, *Penang*, and later upgraded to become MyRTKnet site in the end of 2006 (figure on the left). The figure on the right is the horizontal plot of USMP site positions.

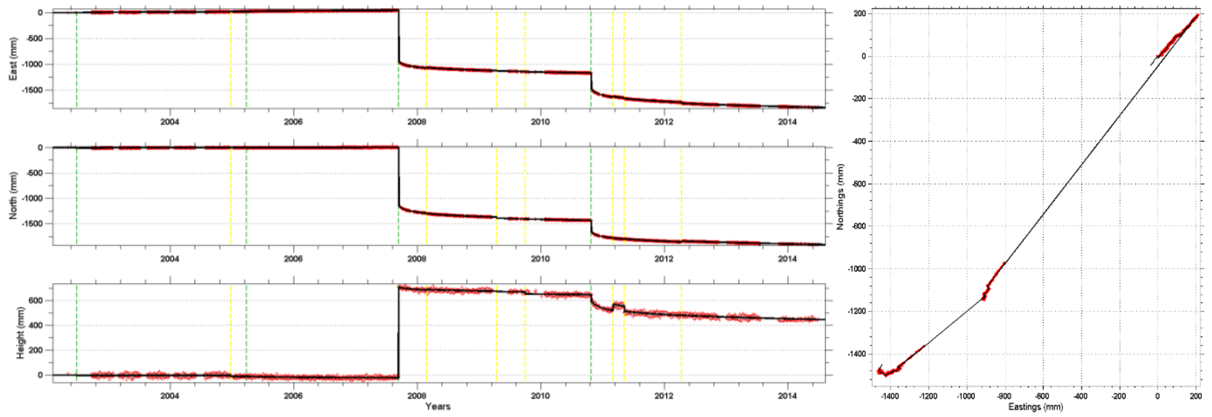

Figure 5: Time-series of station BSAT. This SuGAr site was installed since 2002 at *Bulasat*, South *Pagai* Island (left). The horizontal plot of site positions (right). This site shows high irregular dislocation caused by several great earthquakes during 2004, 2005, 2007 and 2010.

4. GPS DATA ANALYSIS

In this study, the GPS results suggest that the 2004 M_w 9.1 Aceh and 2005 M_w 8.6 Nias earthquakes have changed the course of motion of northwest Peninsular Malaysia, from the southeast to the south-southeast direction. Before the Aceh earthquake, the Peninsular Malaysia moved at a rate of 27-34 mm/yr in 99°-115° azimuth, thereafter, the velocity changed to 13-32 mm/yr in 102°-147° azimuth. The transient site motion continues until the 2012 M_w 8.6 and 8.2 northern Sumatra earthquakes, after which the direction of the velocity vector returns to the orientation prior to 2004 Aceh earthquake at 100°-108°, with a lower displacement rate of 3-12 mm/yr (Table 3). The orientation of the transient velocity event reduces with distance from northern to southern, and from western to eastern Peninsular Malaysia.

Table 3: Comparison of the velocity vector for sites located in Malaysia before 2004/05, 2005 to 2012 and after 2012 earthquakes. The order of sites in Peninsular Malaysia are sorted in high to low latitude. The order of sites in Sabah and Sarawak are sorted in eastwards

Site	Position		Before 2004 - 05		2005 – 2012		After 2012	
	Longitude (°E)	Latitude (°N)	Magnitude (mm/yr)	Azimuth (°)	Magnitude (mm/yr)	Azimuth (°)	Magnitude (mm/yr)	Azimuth (°)
Peninsular Malaysia								
ARAU	100.280	6.450	28	96	13	147	21	108
GETI	102.106	6.226	32	98	25	123	24	103
USMP	100.304	5.358	34	97	16	136	22	105
KUAL	103.139	5.319	32	100	32	102	25	105
LABU*	115.245	5.283	27	115	24	107	24	107
	115.245	5.283						
IPOH*	101.126	4.589	33	94	17	127	25	103
	101.018	4.481						
KUAN*	103.350	3.834	31	97	20	111	29	100
	103.240	4.123						
BEHR	101.517	3.765	31	97	18	119	26	103
KTPK*	101.718	3.171	31	97	19	114	27	103
	101.724	2.993						
UTMJ*	103.640	1.566	31	100	24	105	27	106
	103.797	1.537						
Sabah and Sarawak								
KUCH*	110.195	1.632	29	109	26	110	28	109
	110.425	1.468						
SIBU*	111.843	2.270	24	118	27	112	29	112
	111.673	2.072						
BINT*	113.067	3.262	29	113	27	112	27	112
	113.094	3.240						
MIRI	114.002	4.372	28	109	25	111	26	111
KINA*	116.039	5.905	27	114	28	115	25	108
	116.112	6.039						
TAWA*	117.882	4.263	26	121	26	124	25	123
	117.882	4.263						
SAND	118.121	5.842	30	117	28	120	28	117

Note: Sites that were relocated or upgraded or vector replaced by another nearest site (within a 35 km range after 2005 onwards) as following: BINT replaced by BIN1; IPOH replaced by PUSI; KINA replaced by UMSS; KTPK replaced by UPMS; KUAN replaced by CENE; KUCH replaced by UMAS; LABU replaced by LAB1; SIBU replaced by SIB1; TAWA replaced by MTAW; UTMJ replaced by JHJY.

The existence of significant transient velocities weakens the reliability of existing plate motion models which use Sundaland velocity estimations. To illustrate the misfit in velocity field estimation, a test was performed to compare the estimated vectors in this study with 4 existing global models[1]: (1) MORVEL (DeMets *et al.*, 2010; Argus *et al.*, 2011), (2) CGPS (Prawirodirdjo and Bock, 2004), (3) REVEL (Sella *et al.*, 2002) and (4) GSRM Version 1.2 (Kreemer *et al.*, 2004). The site vectors were estimated for four different periods: (1) 1999.0 – 2014.9 (based on long time-series in ITFR2008); (2) 1999.0 – 2004.9 (before 2004 M9.1 earthquake); (3) 2005.2 – 2012.2 (after 2005 M8.6 and before 2012 M8.6 earthquake); and (4) 2012.2 – 2014.9 (after 2012 M8.6 earthquake). The residual velocity field for all the compared global models are generally similar and one of the residual plot, ITRF2008 (this study)-MORVEL, is shown in Figure 6.

[1] These global models defined the Sundaland plate as a coherent block from Eurasia instead of as a part of Eurasia.

The agreement of MORVEL with the ITRF2008 velocities (1999.0 – 2014.9) are good in the Sarawak, Borneo with an average misfit of 4.2 mm/yr (Figure 6a). However, there are notable misfits and systematic velocity residual patterns in the Mentawai, Sumatra, Sabah (Borneo) and Peninsular Malaysia regions. This is not unexpected for sites that are located close to plate boundaries (*i.e.* Mentawai, Andaman and Sumatra) due to diffuse deformation boundary and localised instability (*i.e.* Sabah). In previous studies, the Peninsular Malaysia has been treated as the undeformed core of the Sundaland plate (Kreemer *et al.*, 2014; Altamimi *et al.*, 2012; Simons *et al.*, 2007), however in Figure 6 it shows a significant model misfit. The largest misfit is in the northwest region of Peninsular Malaysia: from an average misfit of 4.0 mm/yr before 2004 (Figure 6b) to 14.0 mm/yr in 2005-2012 (Figure 6c), and 5.7 mm/yr after 2012 (Figure 6d). Station BKPL in northwest Peninsular Malaysia has experienced one of the largest misfits up to 35.1 mm/yr in 2005-2012. The region characterised by these misfits span the northwest and central-west of Peninsular Malaysia, indicating that the sites in this region also are subjected to intraplate deformation and no longer applicable for derivation of plate rotation vector.

Because of the misfit with the global plate model is, therefore, necessary to estimate a new rotation vector for the Sundaland plate to better understand the interplate and intraplate deformation. In this study, we use the MATLAB-based Euler Pole Calculator (EPC) developed by Goudarzi *et al.*, (2014) to estimate the Euler Pole parameters. The sites having the following criteria were excluded from the definition of rotation vectors of Sundaland plate: (1) sites located close to plate boundary: Andaman, Mentawai and west coast of Sumatra, (2) sites with global plate model misfit exceeding 10 mm/yr, and (3) sites with postseismic deformation (after 2004 Aceh earthquake): northwest Peninsular Malaysia.

The site selection criteria have filtered out all but 10 out of 143 cGPS sites are selected for definition of the rotation vectors of Sundaland plate. The positions, estimated horizontal velocity component and residual of Sundaland fixed for selected 10 sites are listed in Table 4. The coseismic and postseismic deformation from 28 significant earthquakes within the past 16 years (1999 – 2014) have been carefully modelled. The newly defined Euler pole and absolute rotation vector of Sundaland, with comparison with the global models, are shown in Table 5.

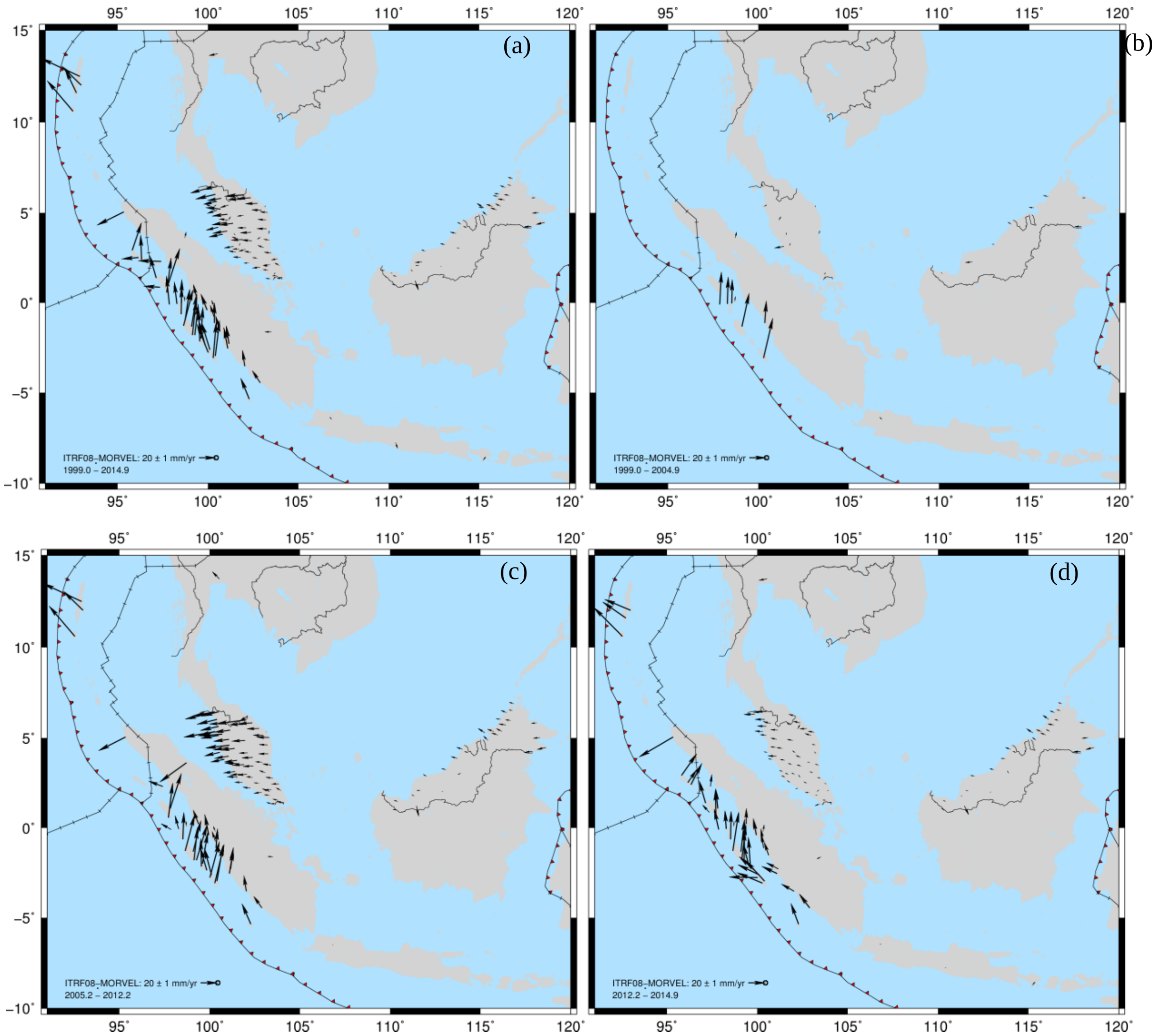

Figure 6: The residuals plot of estimated velocity field with the MORVEL in four different periods: (1) 1999.0 – 2014.9; (2) 1999.0 – 2004.9; (3) 2005.2 – 2012.2; and (4) 2012.2 – 2014.9.

Table 4: Station coordinates of the involved sites, observed ITRF2008 velocities, 1σ uncertainties and Sunda-fixed residuals.

Site	Position		ITRF2008, mm/yr				Residual, mm/yr	
	Longitude (°E)	Latitude (°N)	V_E	V_N	σ_{V_E}	σ_{V_N}	V_E	V_N
BAKO	106.849	-6.491	-6.27	23.28	0.08	0.11	-6.55	3.1
BINT	113.067	3.262	-11.33	27.05	0.05	0.04	1.45	0.83
GETI	102.105	6.226	-4.29	31.45	0.08	0.09	7.45	2.88
KUAL	103.139	5.319	-5.56	31.38	0.03	0.04	6.91	2.09
KUAN	103.350	3.834	-3.77	31.16	0.03	0.04	5.94	3.98
KUCH	110.195	1.632	-9.43	27.64	0.06	0.07	1.32	1.45
MIRI	114.002	4.372	-9.25	26.29	0.03	0.03	1.19	3.31
NTUS	103.680	1.346	-5.78	30.06	0.03	0.04	3.63	2.12
SIBU	111.843	2.270	-11.35	21.43	0.08	0.10	-4.61	0.27
UTMJ	103.640	1.566	-5.32	30.97	0.10	0.10	4.65	2.56

Table 5: Comparison of Euler pole location and absolute rotation vector for the Sundaland plate

Reference frame	Reference	Sites used	Pole Rotation Parameter			Pole Error Ellipse			χ^2
			Lat, °N	Lon, °E	ω°/Myr	$\sigma_{maj/lat}$°	$\sigma_{min/lon}$°	Azimuth°	
REVEL	Sella et al. (2002)	2	38.86	-86.94	0.393 ± 0.062	10.2	0.8	110	0.24
GSRM1.2-NNR	Kreemer *et al.* (2003)	9	47.3	-90.2	0.392 ± 0.008	1.9	0.5	109	3.11
CGPS	Prawirodirdjo & Bock (2004)	2	32.56	-86.80	0.462 ± 0.064	7.0	0.8	113	4.00
ITRF2000	Simons *et al.* (2007)	28	49.0	-94.2	0.336 ± 0.007	1.9	0.3	111	1.03
ITRF2000	DeMets *et al.* (2010)	18	48.5	-93.9	0.326	-	-	-	-
NNR-MORVEL	Argus et al. (2011)	2	50.06	-95.02	0.337 ± 0.020	-	-	-	-
ITRF2008	Altamimi *et al.* (2012)	2	44.25	-87.30	0.388 ± 0.308	-	-	-	-
GSRM2.1-NNR	Kreemer *et al.* (2014)	11*	51.11	-91.75	0.350	-	-	-	-
ITRF2008	**This study**	10	44.16	-87.22	0.349 ± 0.038	6.0	3.3	90	0.07

* Note: The sites velocity used in the Kreemer *et al.*, (2014) were acquired from the literature (*i.e.* Socquet *et al.*, 2006; Simons *et al.*, 2007; Yu *et al.*, 2013).

The impact of great earthquakes in the past decades have changed the preconception of the Peninsular Malaysia as a stable core of Sundaland plate. GPS measurements have shown that the postseismic decay is present during 2004, 2005, 2007, 2010 and 2012 earthquakes, from the west margin of Sundaland up to northwest Peninsular Malaysia, have contaminated the velocity vectors estimated from cGPS sites. Our study shows that there are three key factors that are affected by the determination of Sundaland Euler Pole: (1) the number and location of the sites used to define the rotation vector, (2) different definition of “un-deformed” region within Sundaland plate, and (3) the inclusion of coseismic and postseismic deformation of 2012 M_w 8.6 and 8.2 northern Sumatra earthquakes in vector estimation.

5. CONCLUDING REMARKS

The new velocity field and rotation vector of Sundaland plate presented in this paper are based on 143 regional and 44 IGS network stations. The GPS sites used in this study are solely permanent sites and have a better spatio-temporal coverage in than those used in the previous global velocity models in Sundaland plate. The quantity of GPS sites subset in Malaysia region enabled us to identify the inconsistency of plate vector in a larger scale. The northwest region of Peninsular Malaysia which is normally treated as the undeformed core of Sundaland plate has been shown undergo significant postseismic deformation with model misfit up to an average of 14.0 mm/yr during the interseismic period in 2005-2012. The new results show that the northwest – central-west of Peninsular Malaysia is experiencing higher rotation rate than the south – central-east region.

The series of great earthquakes at the boundary of Indian-Australian and Sundaland plates since 2004 have significantly affected the Sundaland plate velocity field. This study has shown that the extent of the postseismic deformation zone has been underestimated in previous studies. The presence of 2004, 2005, 2007, 2010 and 2012 postseismic events was only successfully detected and modelled with the long time series and densification of the network. A further investigation in relative rotation vector between the Sundaland plate with neighbouring plates (*i.e.* Eurasia, Burma, Australian and Indian plate) are essential to understand the relative plate motion.

ACKNOWLEDGMENTS

The authors would like to thank International GNSS Services (IGS), Department of Surveying & Mapping Malaysia (DSSM), *Badan Informasi Geospasial* (BIG), Indonesian Institute of Science (LIPI), National Mapping and Resource Information Authority (NAMRIA), Scripps Orbit and Permanent Array Centre (SOPAC), California Institute of Technology (Caltech) and Earth Observatory of Singapore (EOS) for maintaining and making the valuable GNSS data and processing parameters available. This paper is also benefited from a review by Sigrun Hreinsdóttir. The maps are generated using Generic Mapping Tools (GMT) software (Wessel and Smith, 1998).

REFERENCES

Altamimi, Z., Métivier, L., and Collilieux, X. (2012). ITRF2008 plate motion model. *Journal of Geophysical Research: Solid Earth*, 117(B7), B07402. doi: 10.1029/2011JB008930

Argus, D. F., Gordon, R. G., and DeMets, C. (2011). Geologically current motion of 56 plates relative to the no-net-rotation reference frame. *Geochemistry, Geophysics, Geosystems*, 12(11), Q11001. doi: 10.1029/2011GC003751

Bird, P. (2003). An updated digital model of plate boundaries. *Geochemistry, Geophysics, Geosystems*, 4(3), 1027. doi: 10.1029/2001GC000252

Bock, Y., Prawirodirdjo, L., Genrich, J. F., Stevens, C. W., McCaffrey, R., Subarya, C., Puntodewo, S.S.O., and Calais, E. (2003). Crustal motion in Indonesia from Global Positioning System measurements. *Journal of Geophysical Research: Solid Earth*, 108(B8), 2367. doi:10.1029/2001JB000324

Boehm, J., Werl, B., and Schuh, H. (2006). Troposphere Mapping Functions for GPS and Very Long Baseline Interferometry from European Centre for Medium-Range Weather Forecasts Operational Analysis Data. *Journal of Research Letter,* 111, B02406. doi: 10.1029/2005JB003629.

Dach, R., Hugentobler, U., Fridez, P., Meindl, M. (Eds) (2007). *Bernese GPS Software Version 5.0*. User manual, Astronomical Institute, University of Bern.

DeMets, C., Gordon, R. G., and Argus, D. F. (2010). Geologically current plate motions. *Geophysical Journal International*, 181(1), 1-80. doi: 10.1111/j.1365-246X.2009.04491.x

Duputel, Z., Kanamori, H., Tsai, V. C., Rivera, L., Meng, L., Ampuero, J.-P. and Stock, J. M. (2012). The 2012 Sumatra great earthquake sequence. *Earth and Planetary Science Letters* 351–352(0): 247-257. doi: 10.1016/j.epsl.2012.07.017

Goudarzi, M. A., Cocard, M., and Santerre, R. (2014). EPC: Matlab software to estimate Euler pole parameters. *GPS Solutions*, *18*(1), 153-162. doi:10.1007/s10291-013-0354-4

Kreemer, C., Holt, W. E., and Haines, A. J. (2003). An integrated global model of present-day plate motions and plate boundary deformation. *Geophysical Journal International*, 154(1), 8-34. doi: 10.1046/j.1365-246X.2003.01917.x

Kreemer, C., Blewitt, G., and Klein, E. C. (2014). A geodetic plate motion and Global Strain Rate Model. *Geochemistry, Geophysics, Geosystems, 15*(10), 3849-3889. doi:10.1002/2014GC005407

Musa, T. A., Amir, S., Othman, R., Ses, S., Omar, K., Abdullah, K., Lim, S., and Rizos, C. (2011). GPS meteorology in a low-latitude region: Remote sensing of atmospheric water vapor over the Malaysian Peninsula. *Journal of Atmospheric and Solar-Terrestrial Physics*, 73(16), 2410-2422. http://dx.doi.org/10.1016/j.jastp.2011.08.014

Prawirodirdjo, L. and Bock, Y. (2004). Instantaneous global plate motion model from 12 years of continuous GPS observations. *Journal of Geophysical Research: Solid Earth*, 109(B8): B08405.

Scherneck, H.-G. (1991). A parametrized solid Earth tide mode and ocean loading effects for global geodetic base-line measurements. *Geophys. J. Int.*, 106(3):677-694.

Sella, G. F., Dixon, T.H., and Mao, A. (2002). REVEL: A model for Recent plate velocities from space geodesy. *Journal of Geophysical Research: Solid Earth*, 107(B4): ETG 11-1 – ETG 11-30.
Simons, W. J. F., Socquet, A., Vigny, C., Ambrosius, B. A. C., Haji Abu, S., Promthong, C., Subarya, C., Sarsito, D. A., Matheussen, S., Morgan, P. and Spakman, W. (2007). A decade of GPS in Southeast Asia: Resolving Sundaland motion and boundaries. *Journal of Geophysical Research: Solid Earth, 112*(B6), B06420. doi:10.1029/2005JB003868
Socquet, A., Vigny, C., Chamot-Rooke, N., Simons, W., Rangin, C., and Ambrosius, B. (2006). India and Sunda plates motion and deformation along their boundary in Myanmar determined by GPS. *Journal of Geophysical Research: Solid Earth*, *111*(B5), B05406. doi:10.1029/2005JB003877
Wessel, P., and Smith, W.H. (1998). New, improved version of Generic Mapping Tools released. *Eos, Trans. Am. Geophys. Union*, 79 (47), 579–579. doi: 10.1029/98EO00426

BIOGRAPHICAL NOTES

Yong Chien Zheng is a PhD candidate in National School of Surveying, University of Otago with research interest in geodesy, geodynamics and seismological study. He obtained a Degree of Engineering (Geomatics) and Master of Science (Satellite Surveying) from Universiti Teknologi Malaysia.

Paul Denys is a senior lecturer at the National School of Surveying, University of Otago. He joined the School in June 1995. He holds a Doctorate from the University of Newcastle, United Kingdom and a MSurv degree at Otago University. Since joining Otago University, his primary research focus has involved projects on the deformation of the South Island, vertical uplift of the Southern Alps, the effect of and integration of deformation events (*e.g.* earthquakes) on geodetic infrastructure and decoupling vertical land movement at tide gauge stations.

Christopher Pearson is a senior lecturer at the National School of Surveying, University of Otago. He completed his PhD from the University of Otago, New Zealand in 1991 and then spent a year working on a post-doc at Columbia University. He is currently teaching and conducting research in areas of Geodesy, Crustal deformation, GPS and least square adjustments.

CONTACTS

Yong Chien Zheng
National School of Surveying
University of Otago
PO Box 56
Dunedin 9054
NEW ZEALAND
Email: yong.chienzheng@gmail.com
Web site: http://www.otago.ac.nz/surveying/

Paul Denys
National School of Surveying
University of Otago
PO Box 56
Dunedin 9054
NEW ZEALAND
Email: paul.denys@otago.ac.nz
Web site: http://www.otago.ac.nz/surveying/

Christopher Pearson
National School of Surveying
University of Otago
PO Box 56
Dunedin 9054
NEW ZEALAND
Email: chris.pearson@otago.ac.nz
Web site: http://www.otago.ac.nz/surveying/